Supporting Information

Effect of ligand denticity on the nitric oxide reactivity of its cobalt(II) complexes

Hemanta Deka[a], Somnath Ghosh[a], Soumen Saha[a], Kuldeep Gogoi[a] and Biplab Mondal,*[a]

[a] *Department of Chemistry, Indian Institute of Technology Guwahati, Assam -781039, India.*

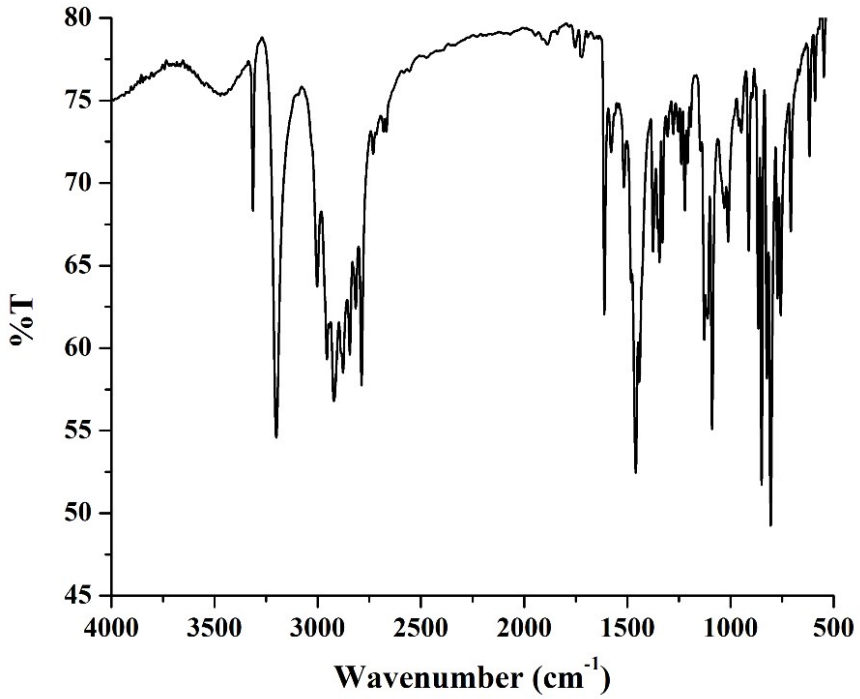

Figure S1. FT-IR spectrum of ligand $\mathbf{L_1}$ in KBr pellet.

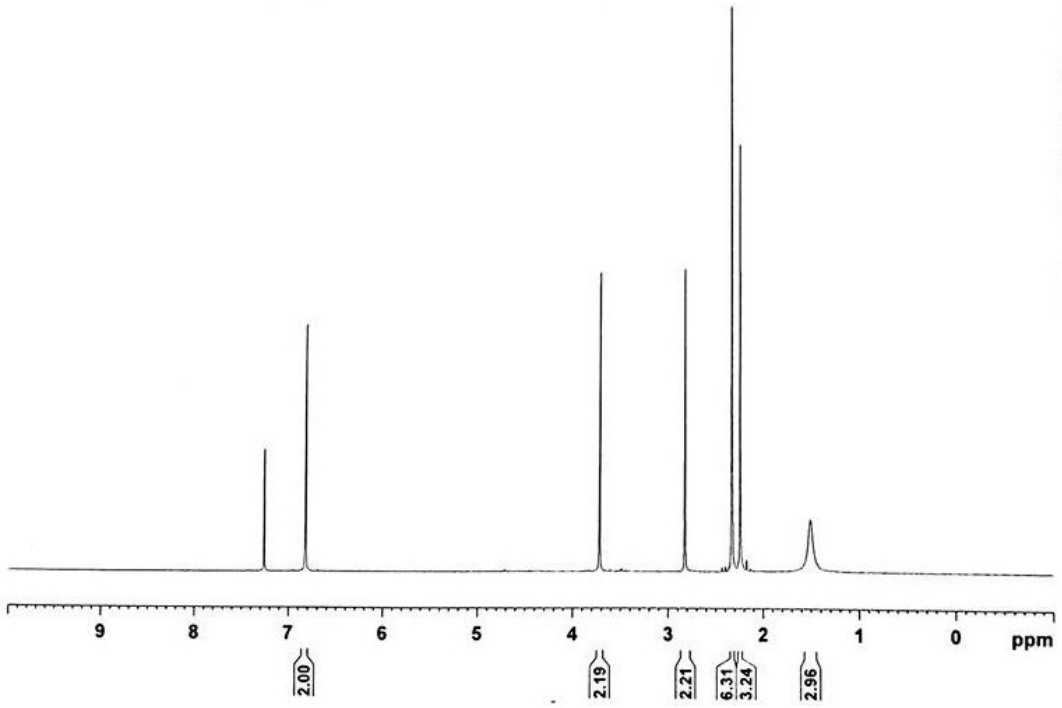

Figure S2. ^{1}H NMR spectrum of $\mathbf{L_1}$ in $CDCl_3$.

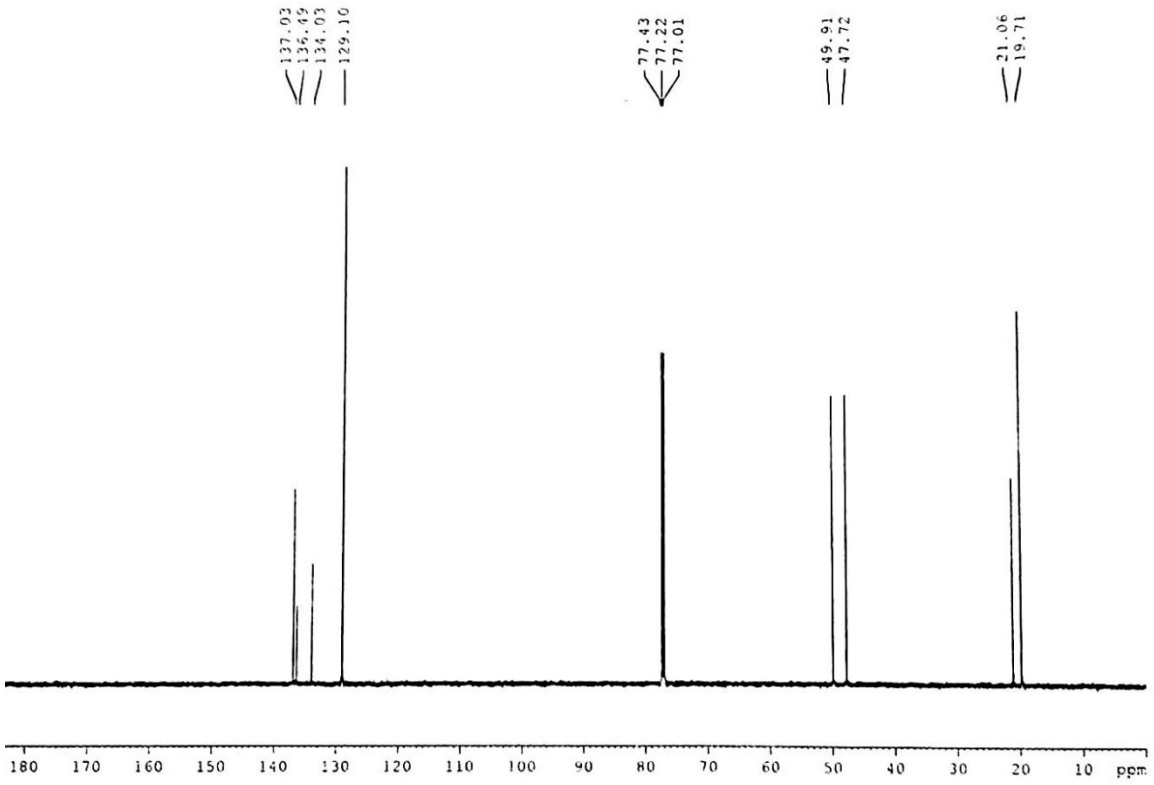

Figure S3. ^{13}C NMR spectrum of $\mathbf{L_1}$ in $CDCl_3$.

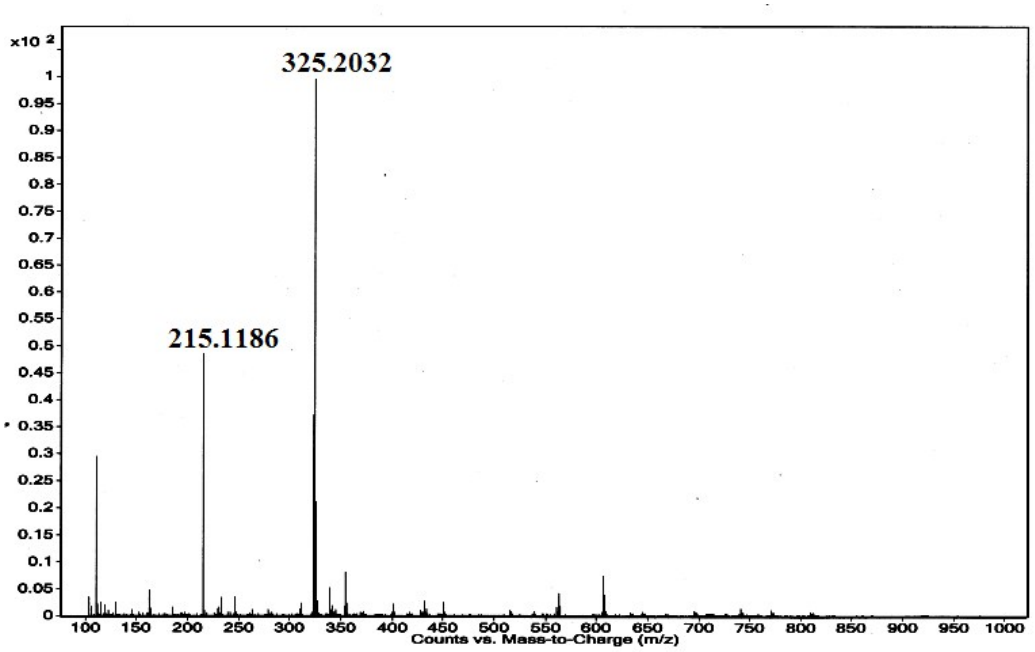

Figure S4. ESI-mass spectrum of $\mathbf{L_1}$ in methanol.

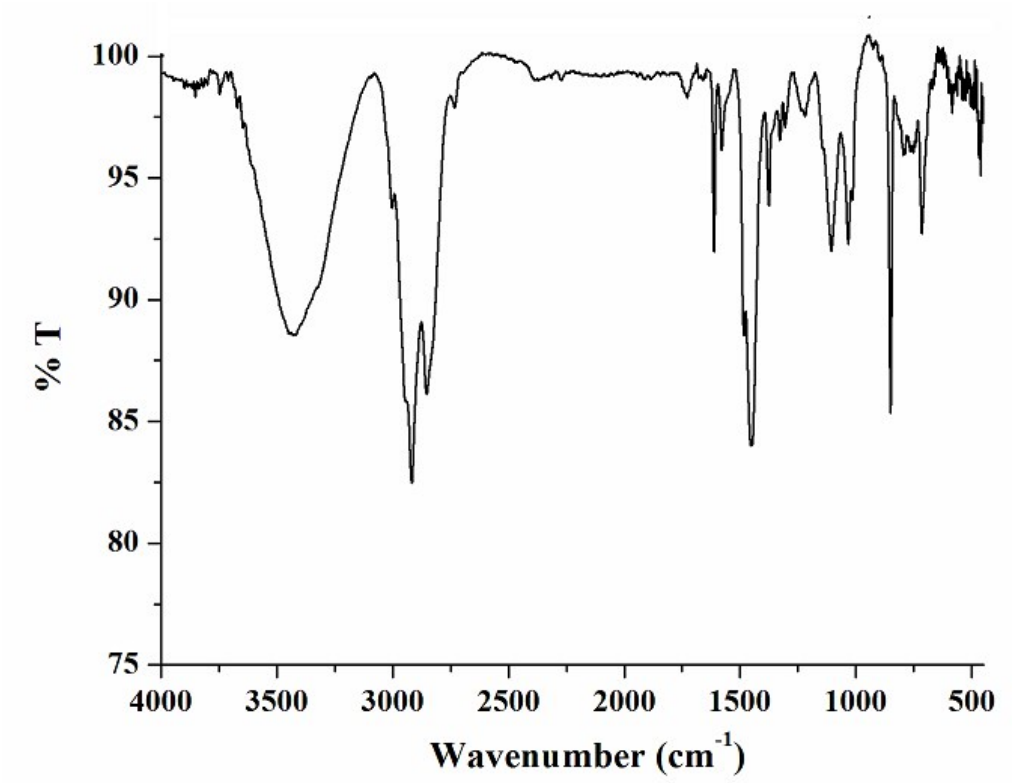

Figure S5. FT-IR spectrum of ligand $\mathbf{L_2}$ in KBr pellet.

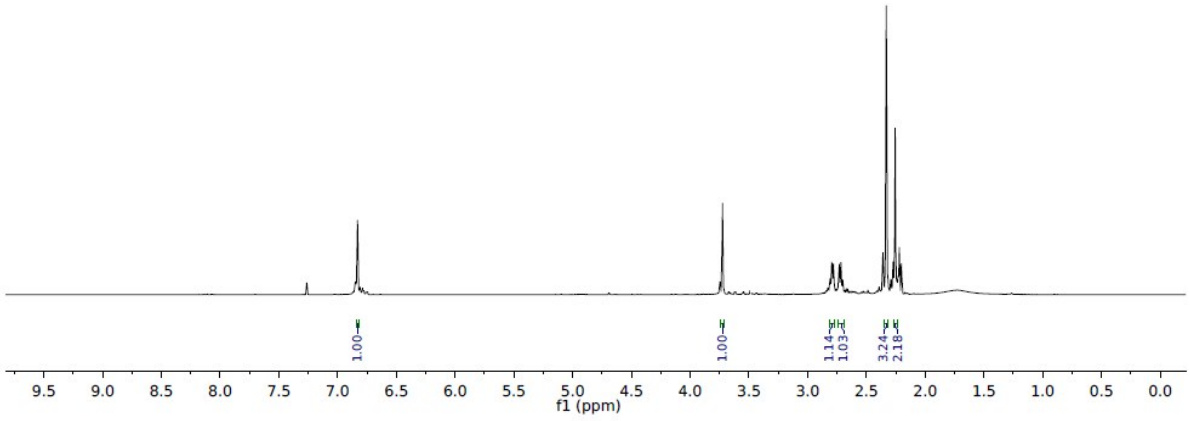

Figure S6. ^{1}H NMR spectrum of $\mathbf{L_2}$ in $CDCl_3$.

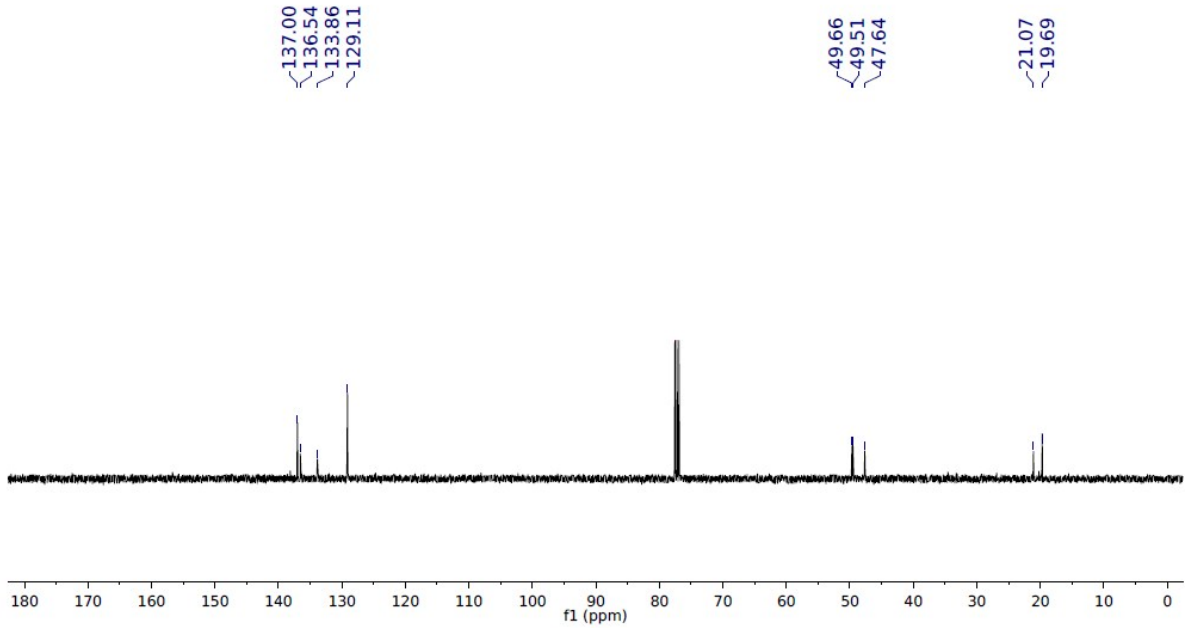

Figure S7. ^{13}C NMR spectrum of $\mathbf{L_2}$ in $CDCl_3$.

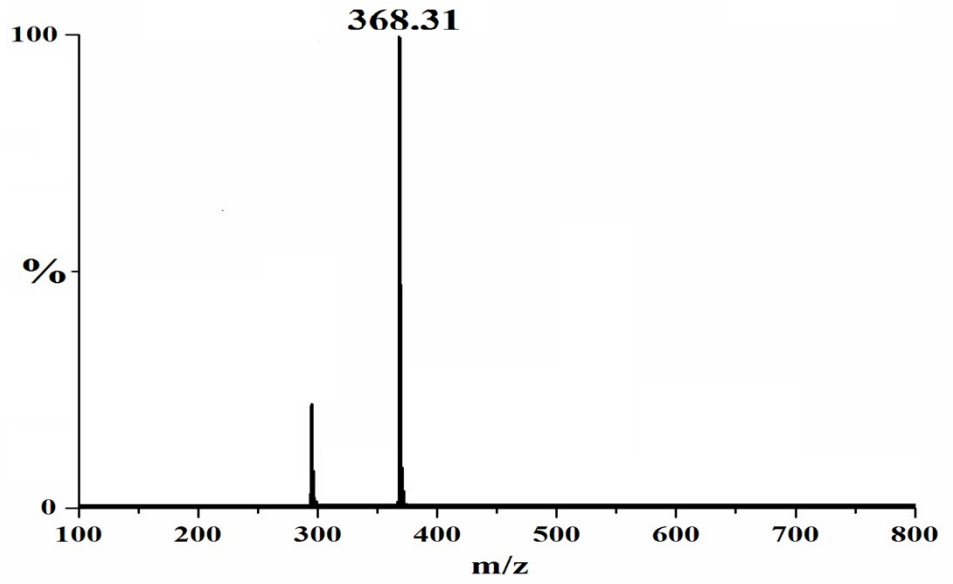

Figure S8. ESI-mass spectrum of $\mathbf{L_2}$ in methanol.

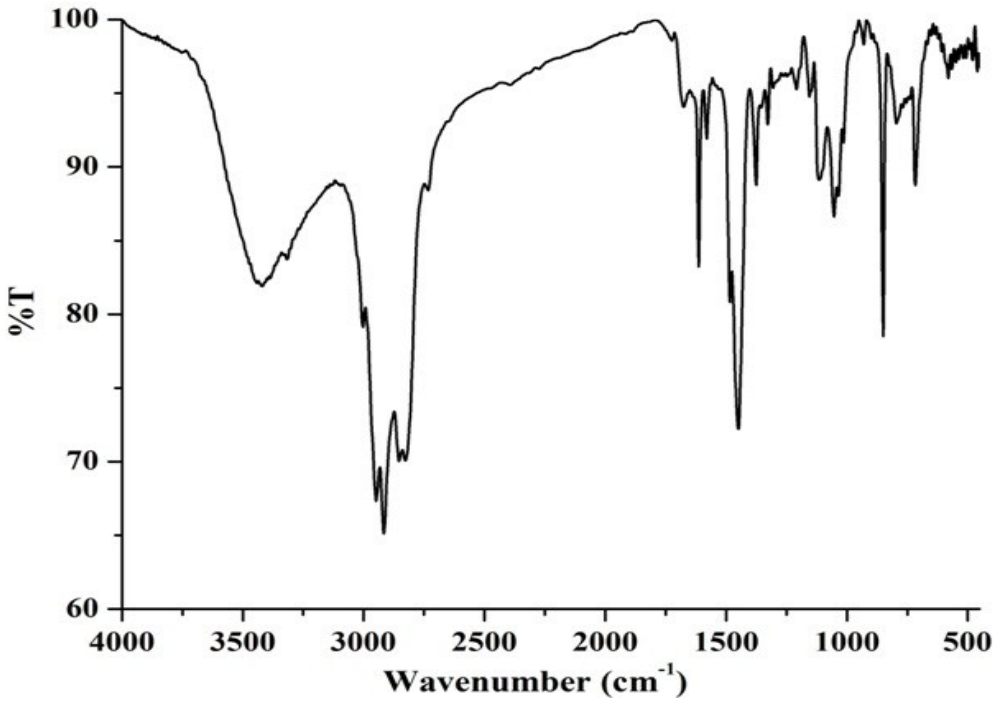

Figure S9. FT-IR spectrum of ligand $\mathbf{L_3}$ in KBr pellet.

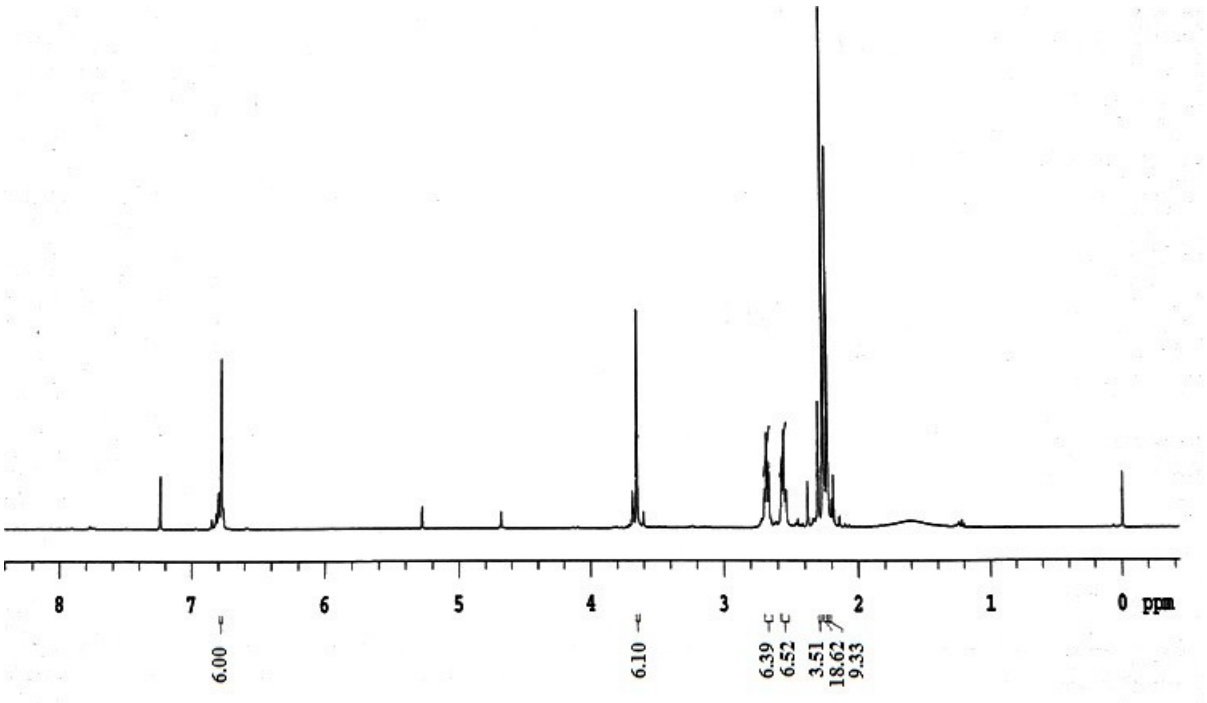

Figure S10. ^{1}H NMR spectrum of $\mathbf{L_3}$ in $CDCl_3$.

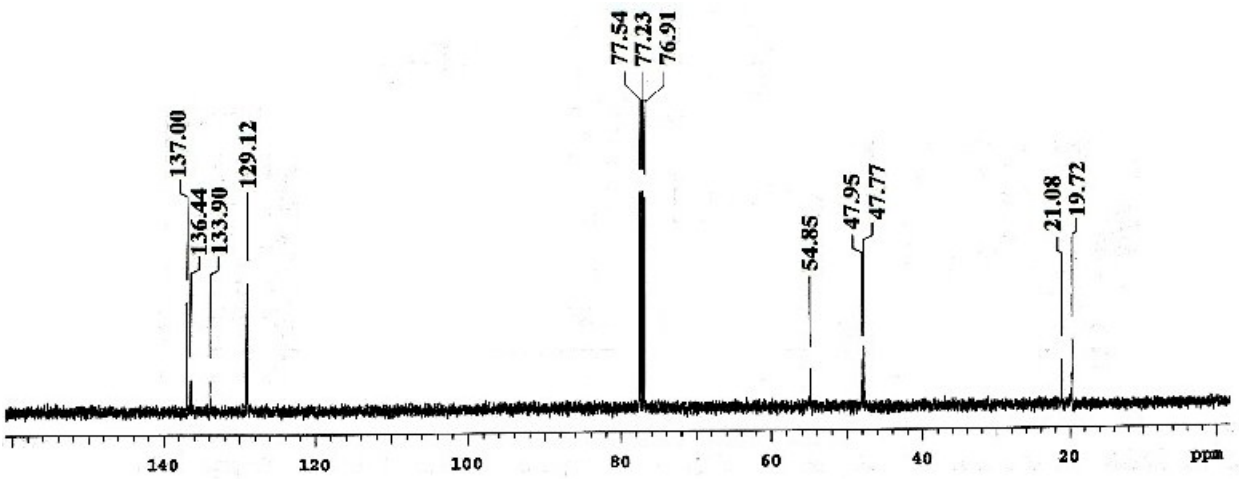

Figure S11. ^{13}C NMR spectrum of $\mathbf{L_3}$ in $CDCl_3$.

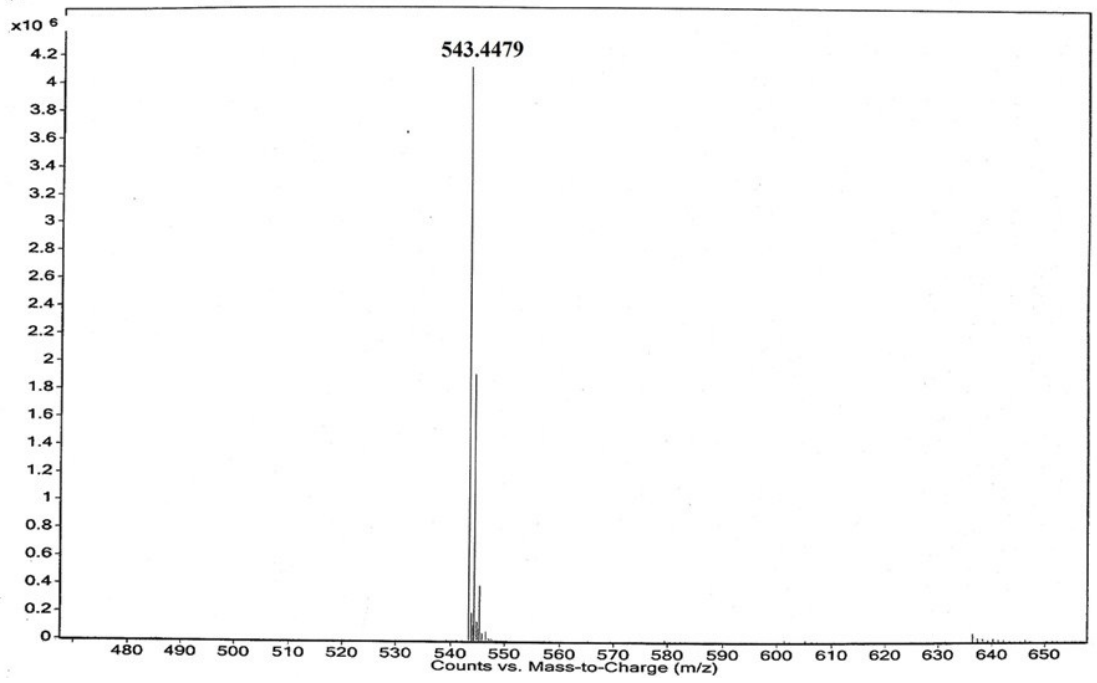

Figure S12. ESI-mass spectrum of $\mathbf{L_3}$ in methanol.

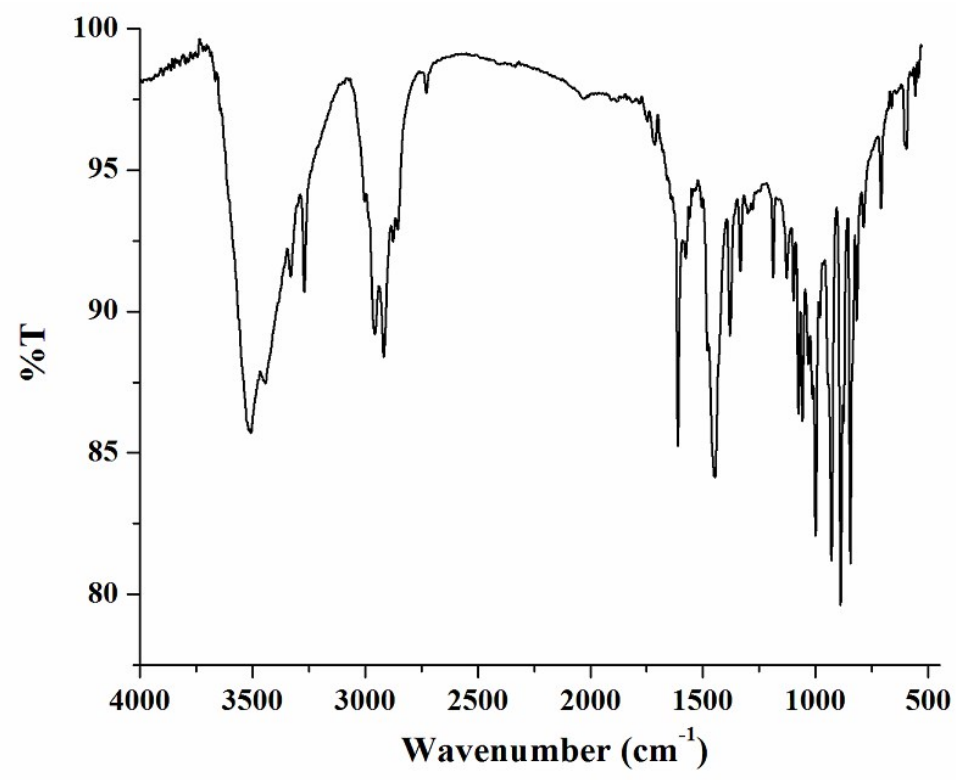

Figure S13. FT-IR spectrum of complex **1** in KBr pellet.

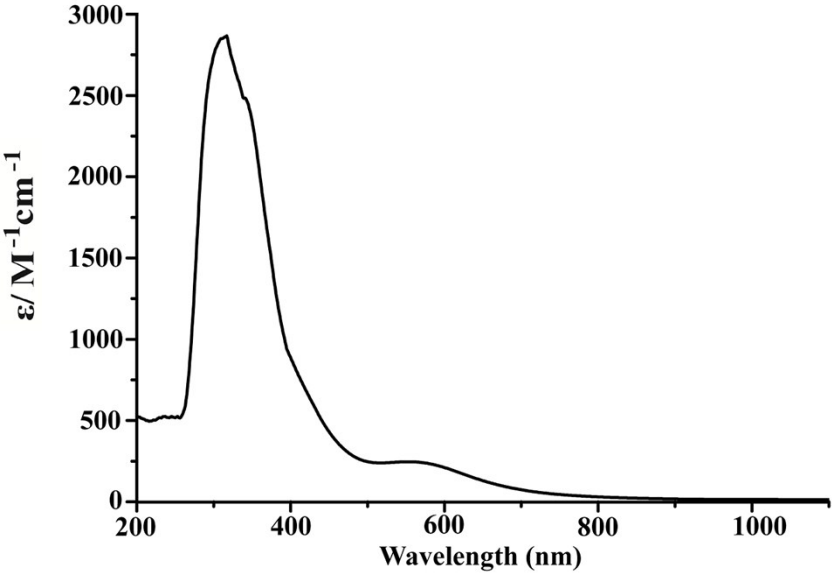

Figure S14. UV-visible spectrum of complex **1** in methanol.

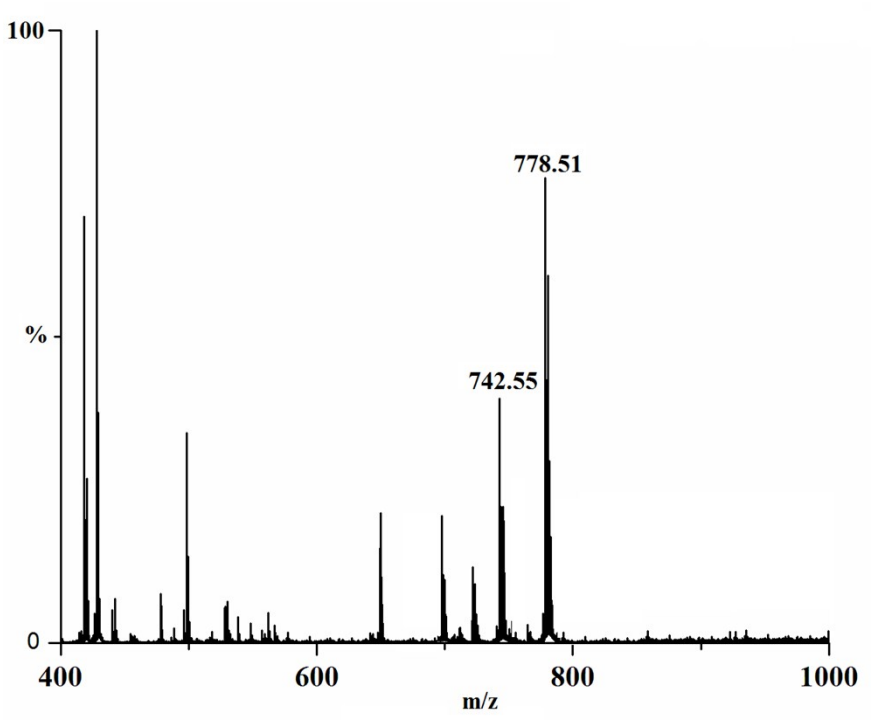

Figure S15. ESI-mass spectrum of complex **1** in methanol.

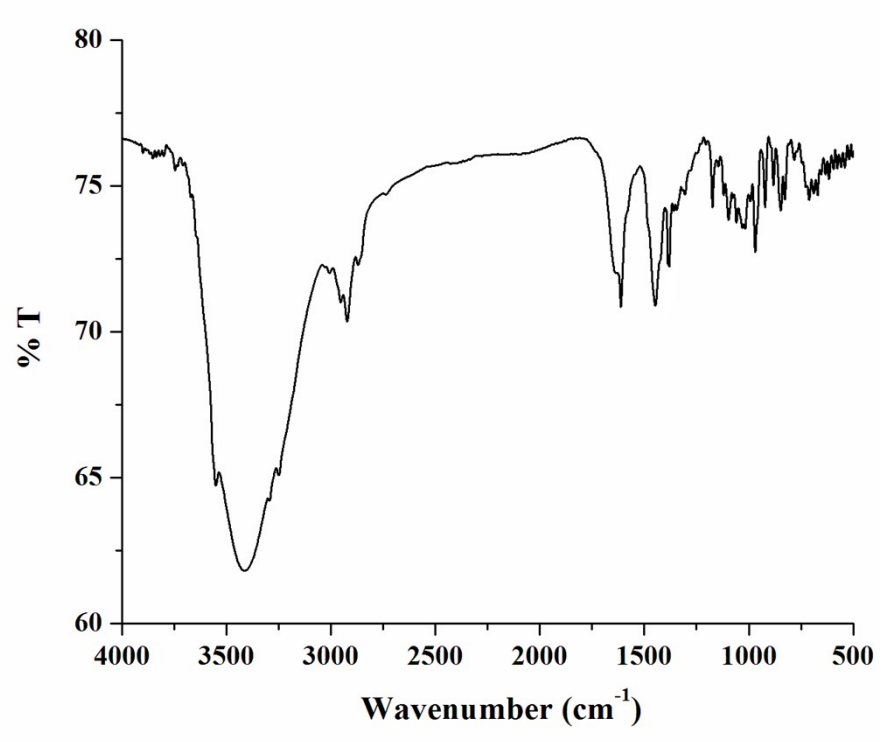

Figure S16. FT-IR spectrum of complex **2** in KBr pellet.

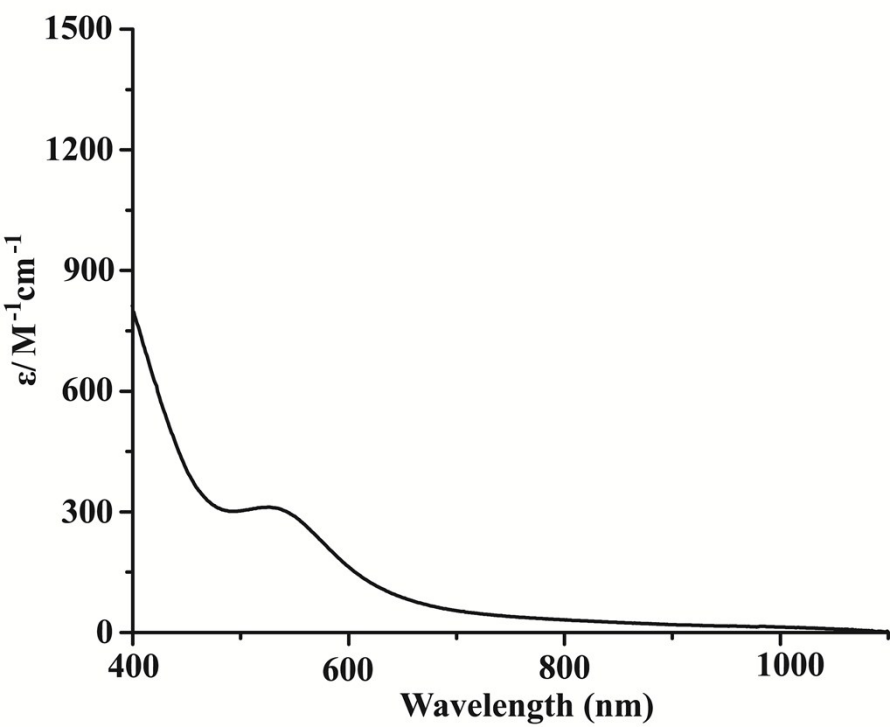

Figure S17. UV-visible spectrum of complex **2** in methanol.

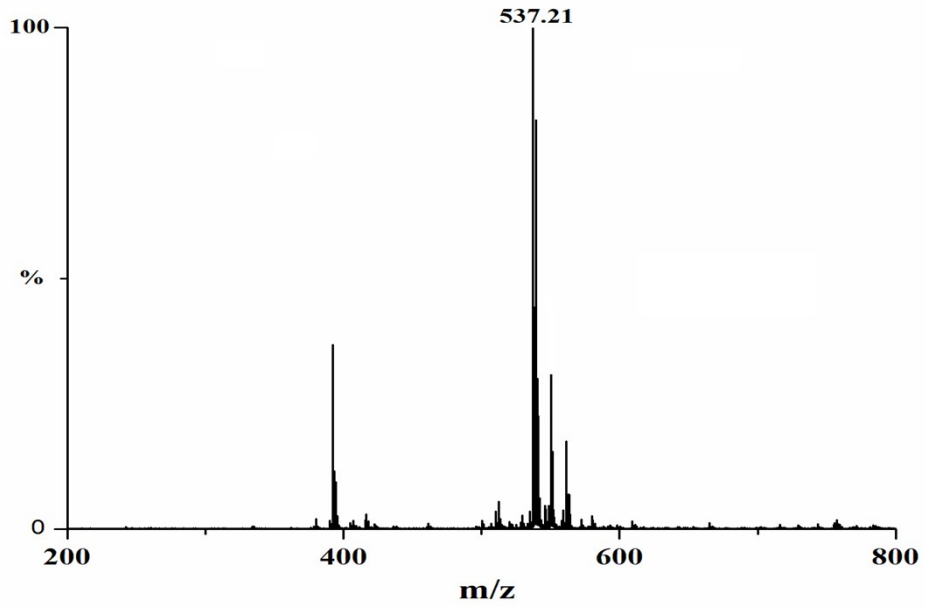

Figure S18. ESI-mass spectrum of complex **2** in acetonitrile.

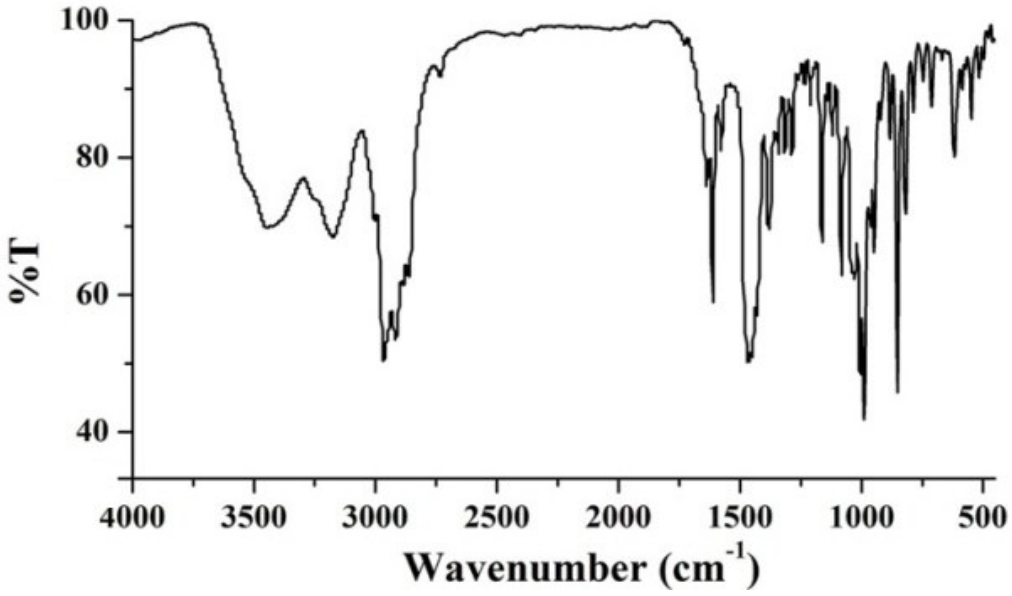

Figure S19. FT-IR spectrum of complex **3** in KBr pallet.

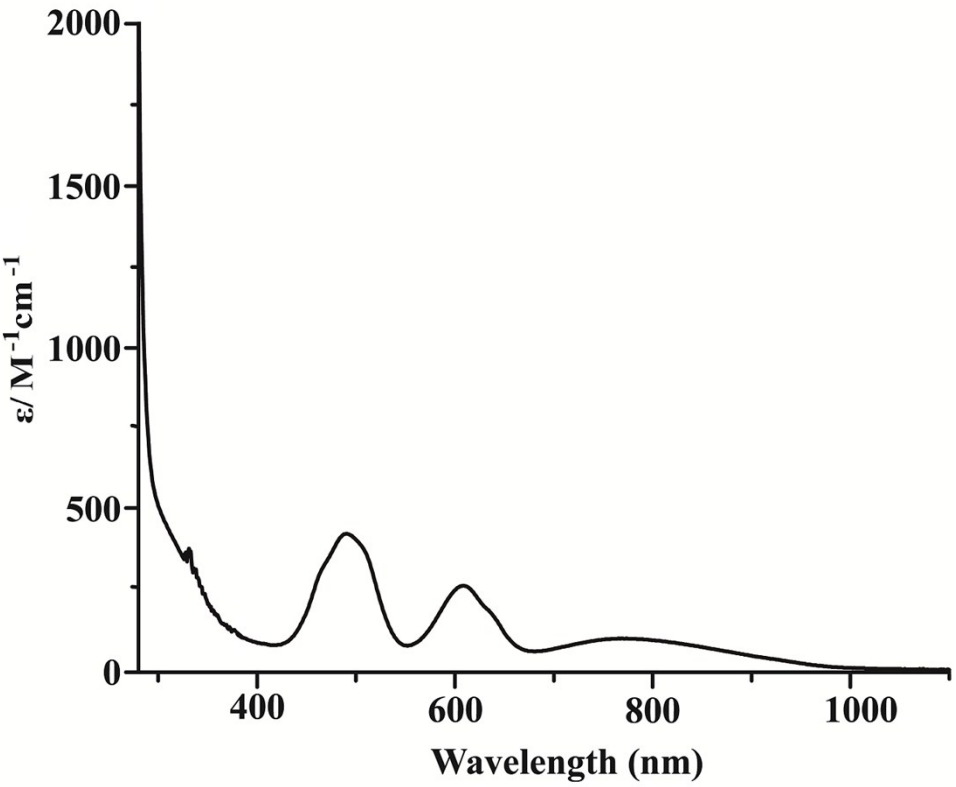

Figure S20. UV-visible spectrum of complex **3** in methanol.

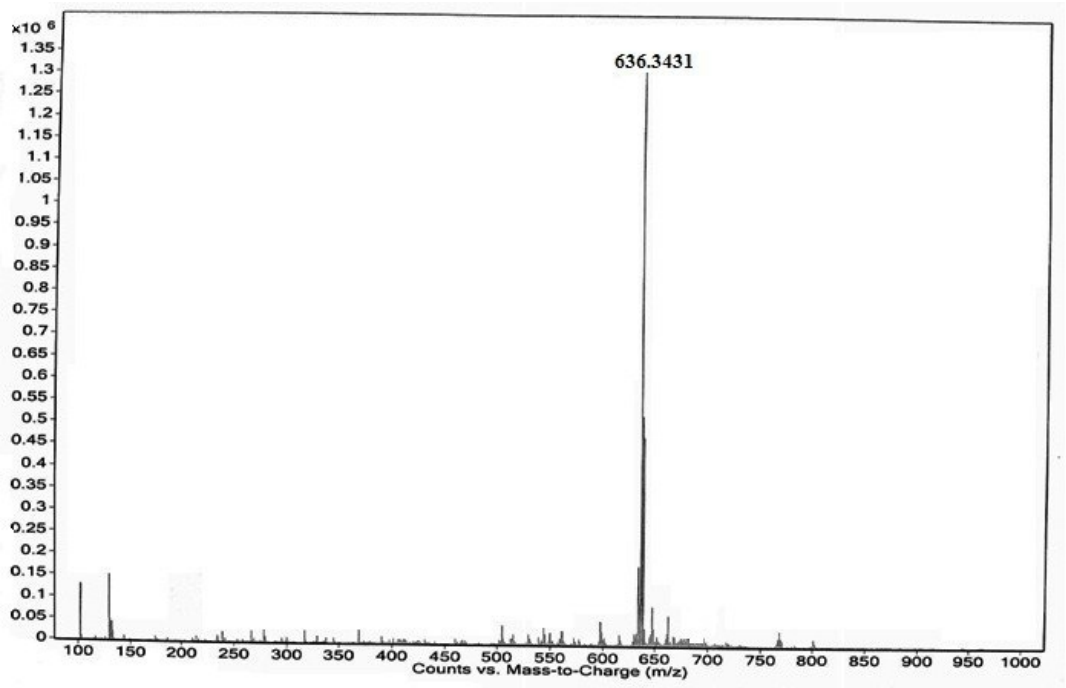

Figure S21. ESI-mass spectrum of Complex **3** in methanol.

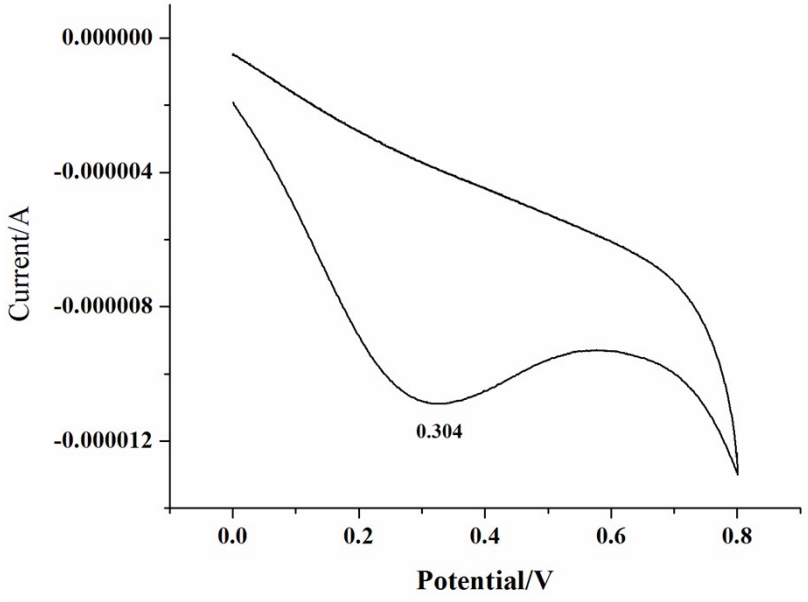

Figure S22. Cyclic Voltammogram of Complex **1,** positive scan.

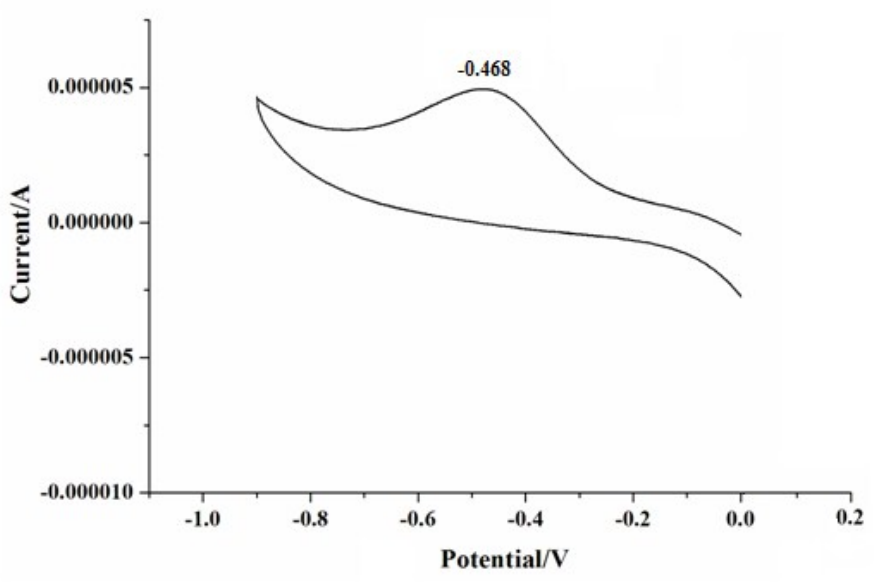

Figure S23. Cyclic Voltammogram of Complex **1,** negative scan.

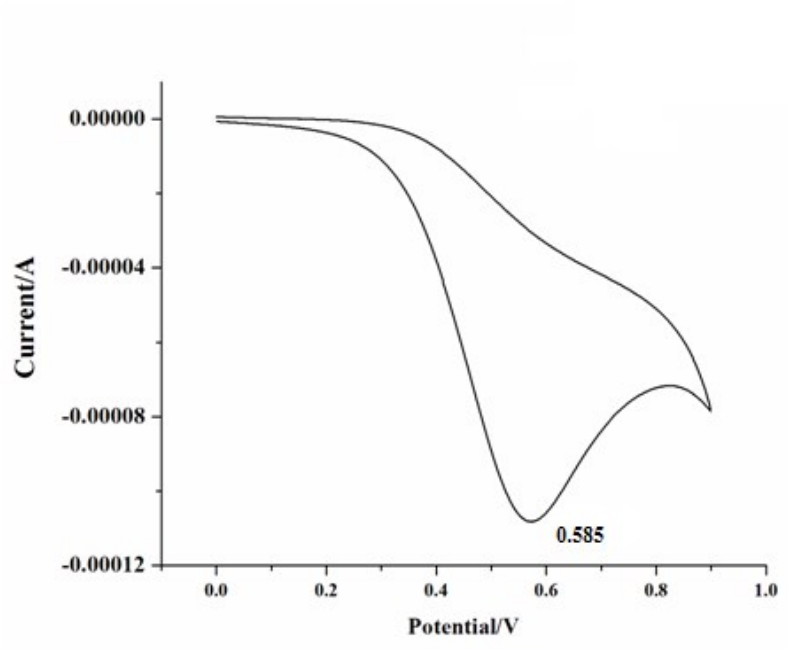

Figure S24. Cyclic Voltammogram of Complex **2,** positive scan.

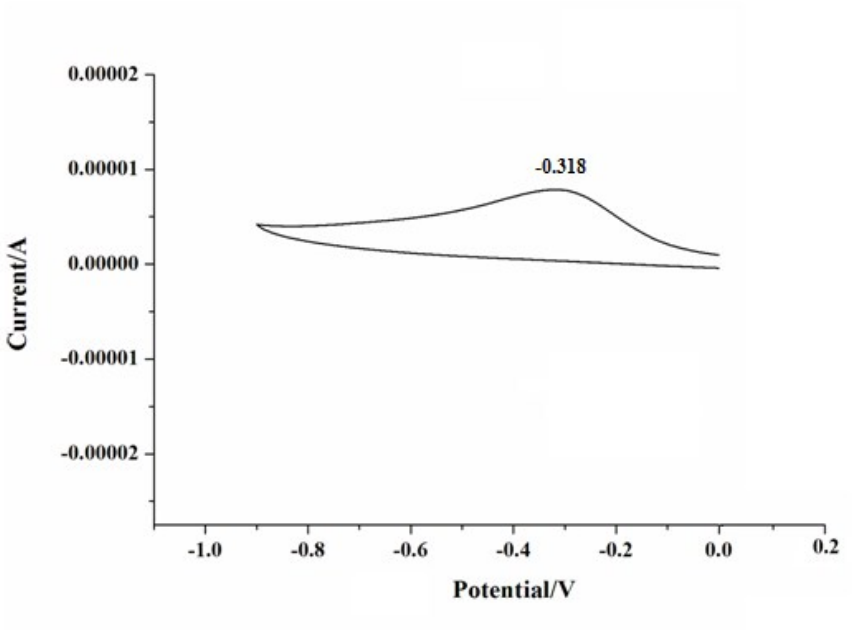

Figure S25. Cyclic Voltammogram of Complex **2,** negative scan.

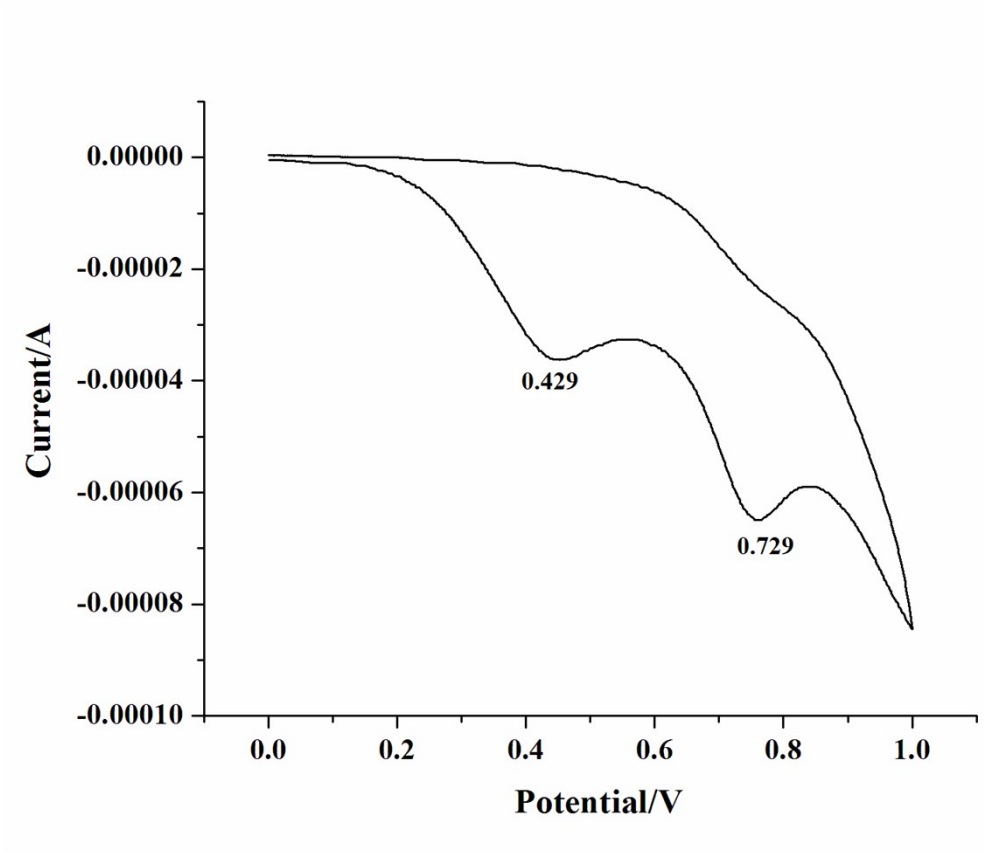

Figure S26. Cyclic Voltammogram of Complex **3,** positive scan.

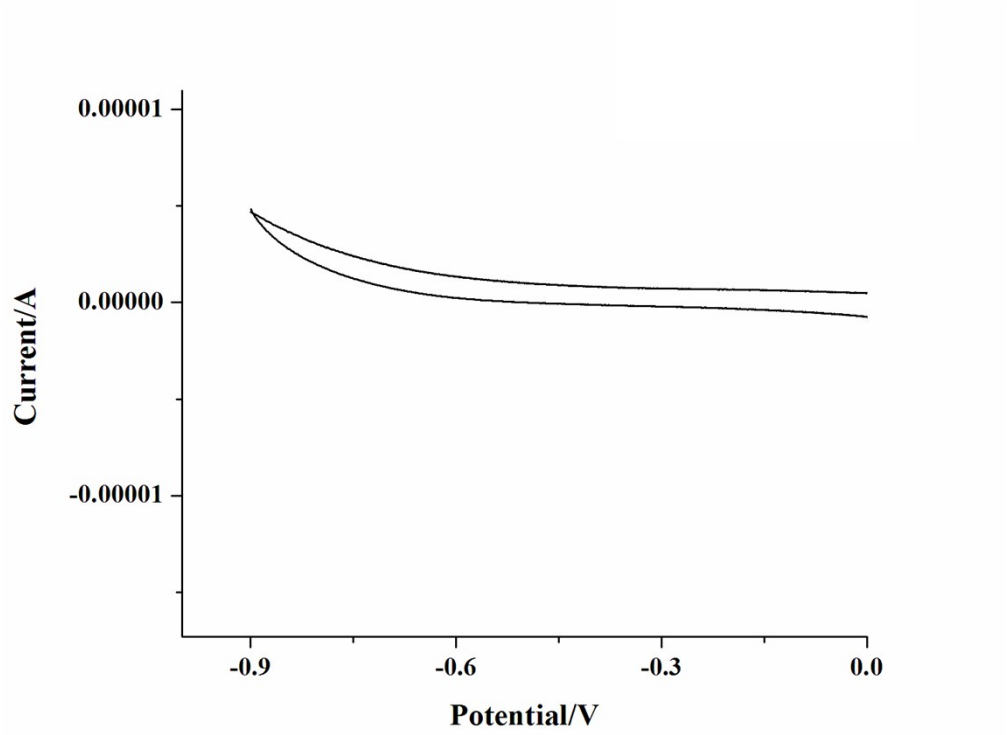

Figure S27. Cyclic Voltammogram of Complex **3,** negative scan.

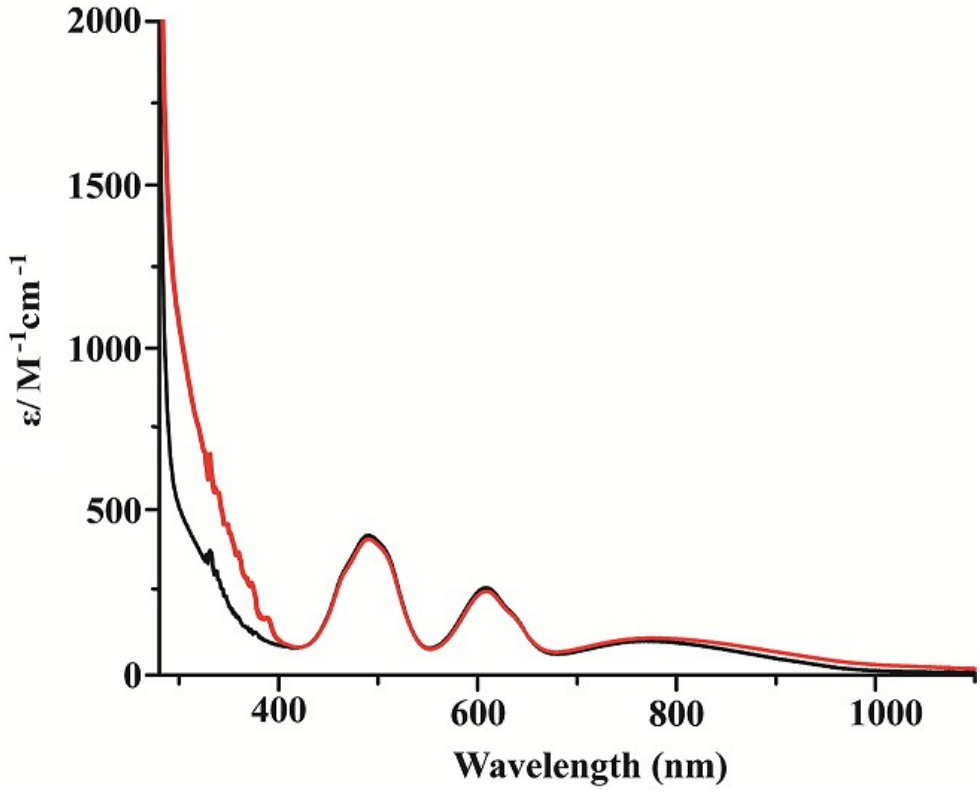

Figure S28. UV-visible spectra of complex **3** (black line) and upon addition of excess NO (red line) in methanol under argon atmosphere.

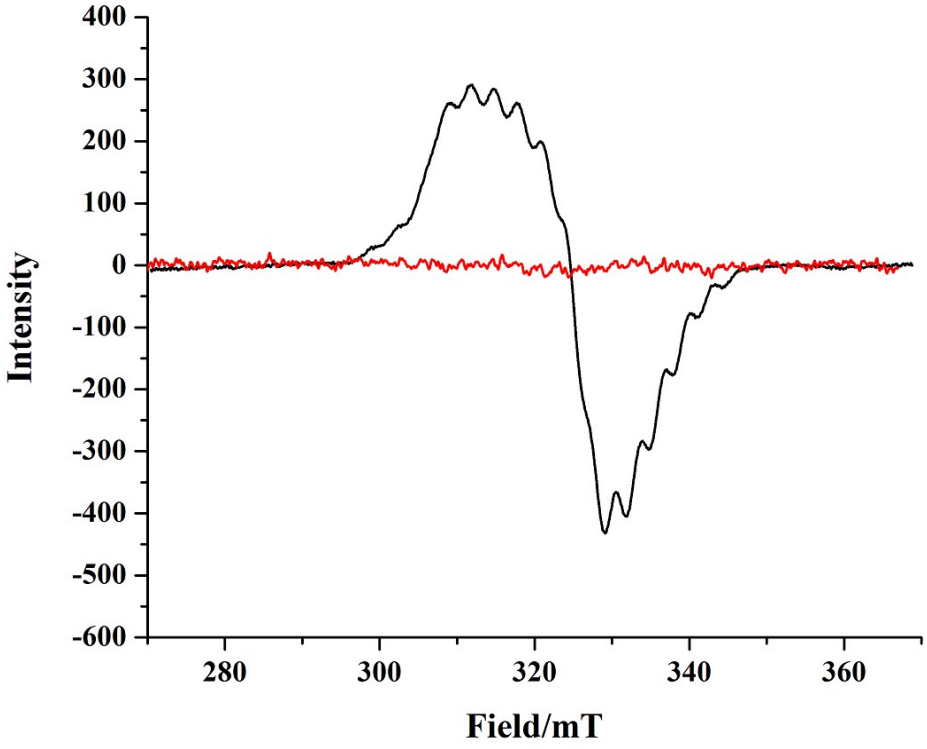

Figure S29. X-band EPR spectra of complex **1** (black line) and upon addition of excess NO (red line) in methanol under argon atmosphere.

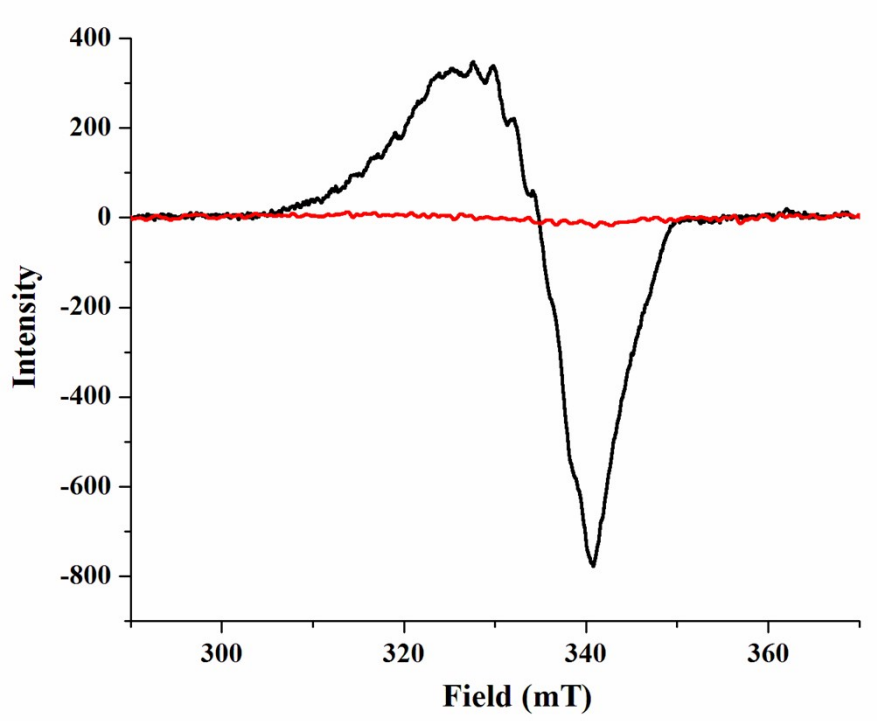

Figure S30. X-band EPR spectra of complex **2** (black line) and upon addition of excess NO (red line) in methanol under argon atmosphere.

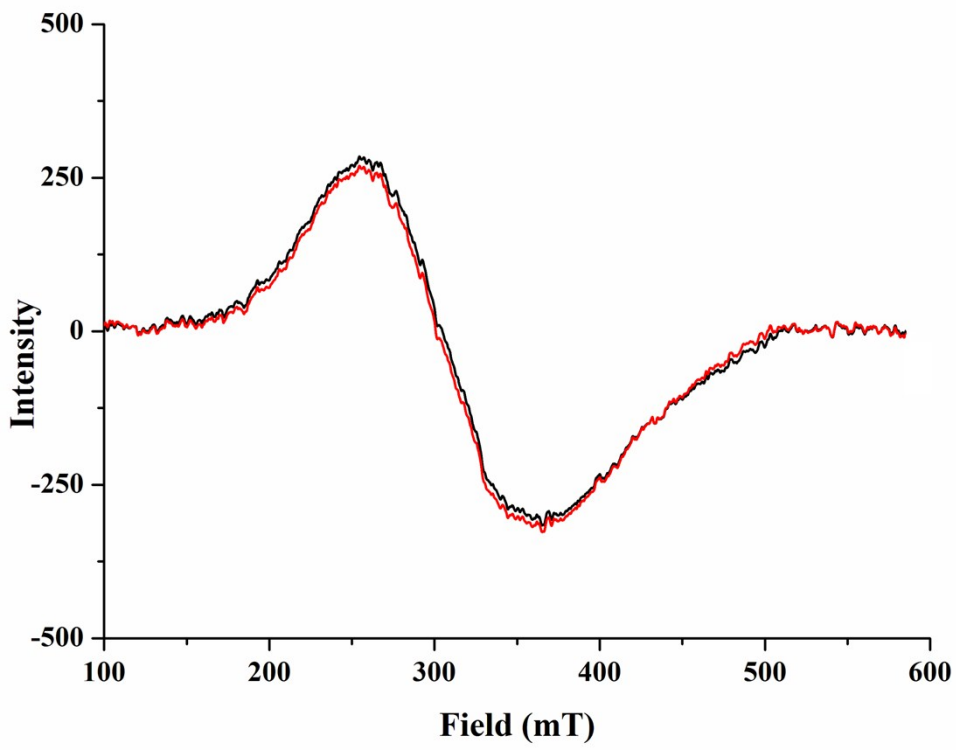

Figure S31. X-band EPR spectra of complex **3** (black line) and upon addition of excess NO (red line) in methanol under argon atmosphere.

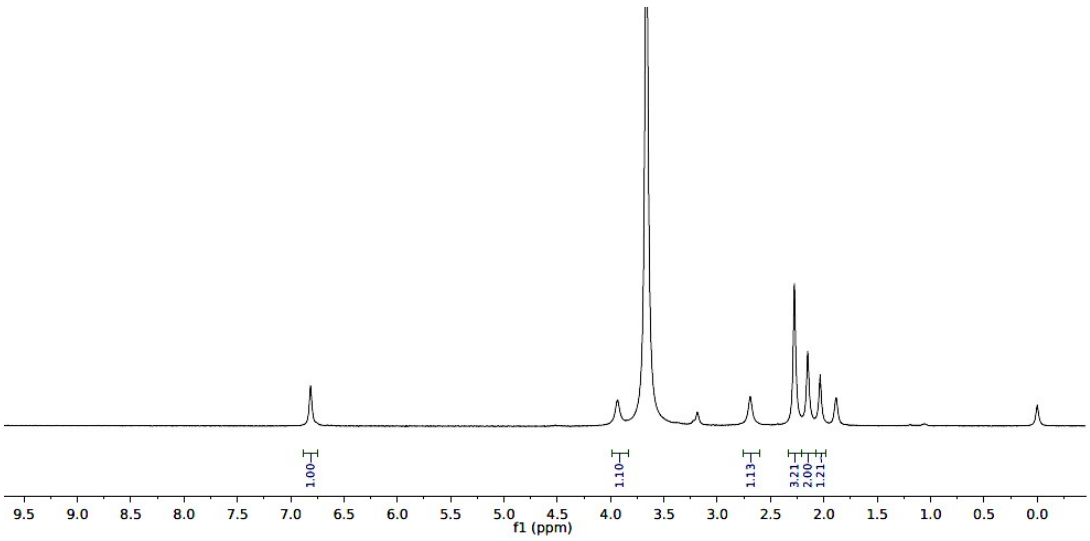

Figure S32. ^{1}H NMR spectrum of complex **4a** in CD_3OD.

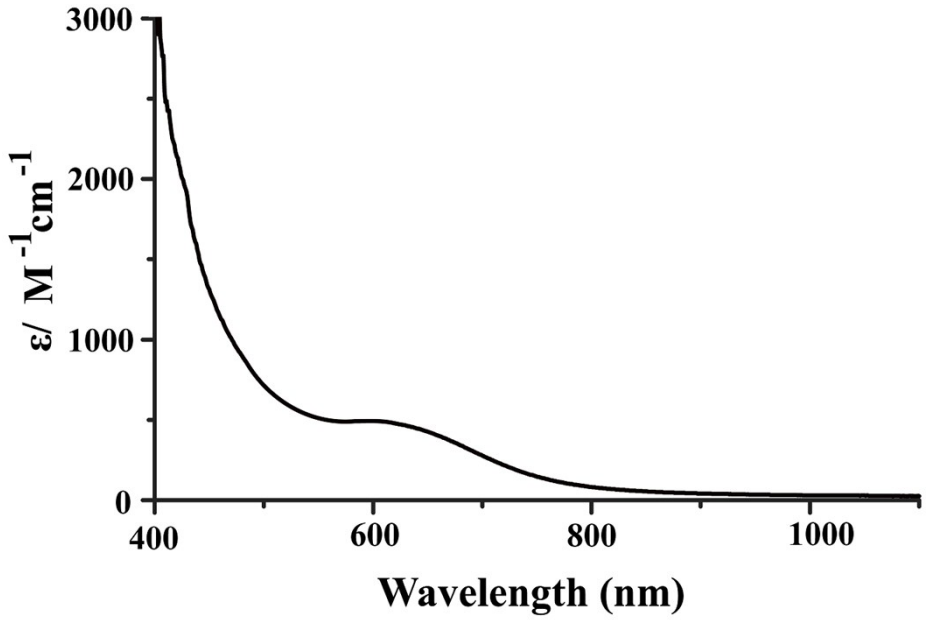

Figure S33. UV-visible spectrum of complex **4a** in methanol.

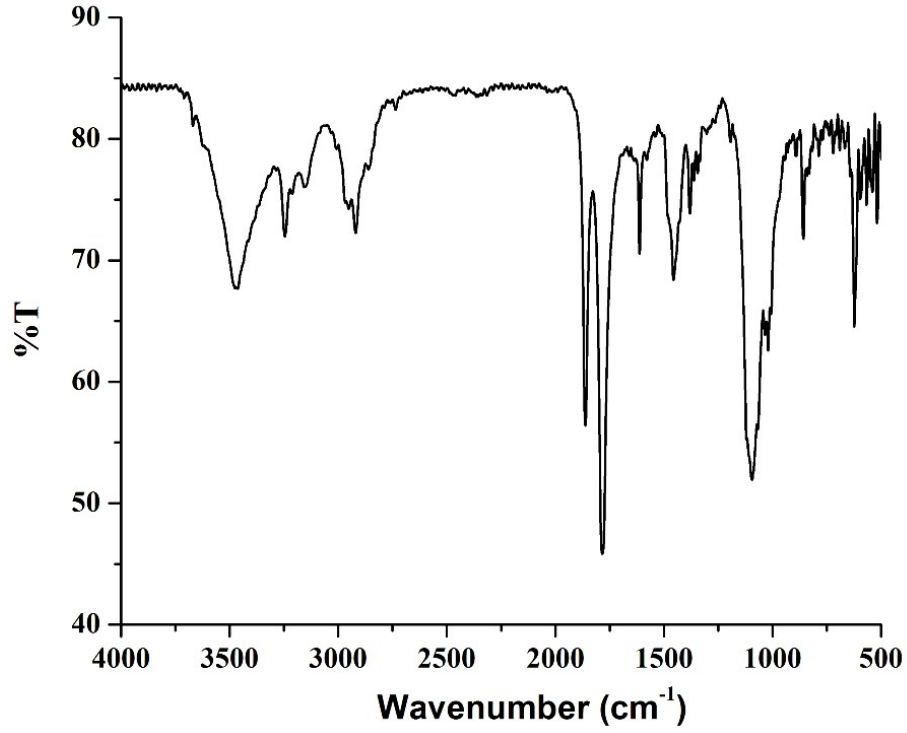

Figure S34. FT-IR spectrum of complex **4b** in KBr pellet.

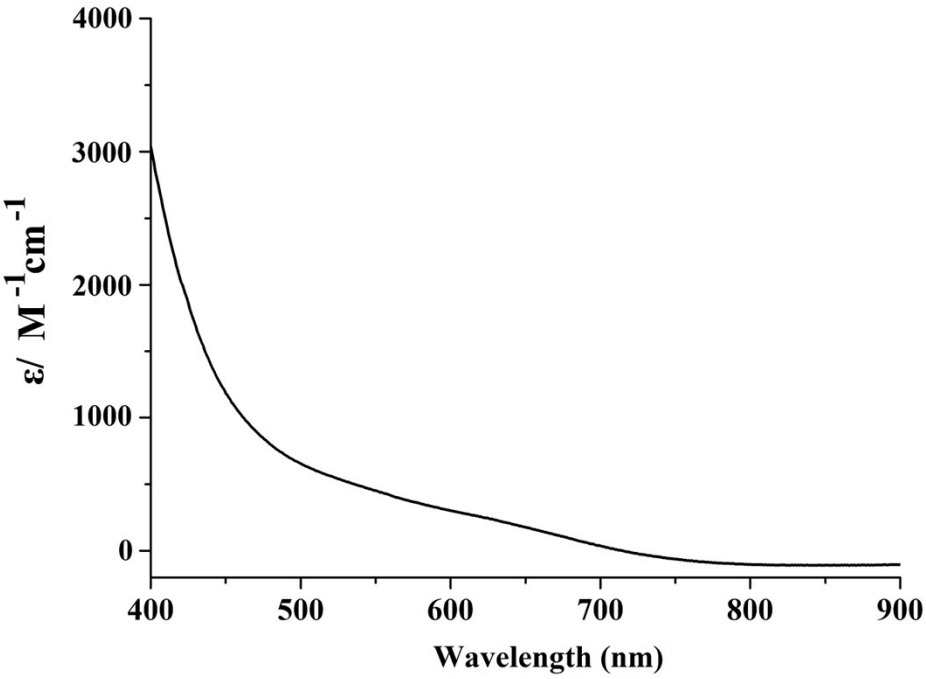

Figure S35. UV-visible spectrum of complex **4b** in methanol. Inset shows the d-d transition region.

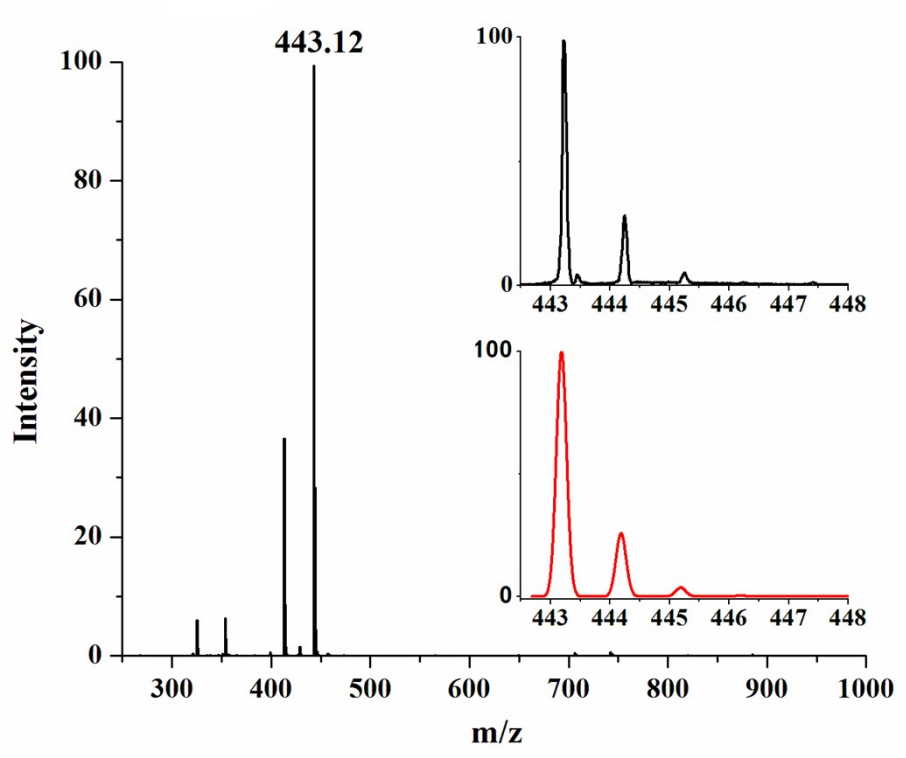

Figure S36. ESI-mass spectrum of complex **4a** in acetonitrile. Inset shows isotopic distribution pattern. Black line corresponds experimental and red line corresponds simulated mass spectra.

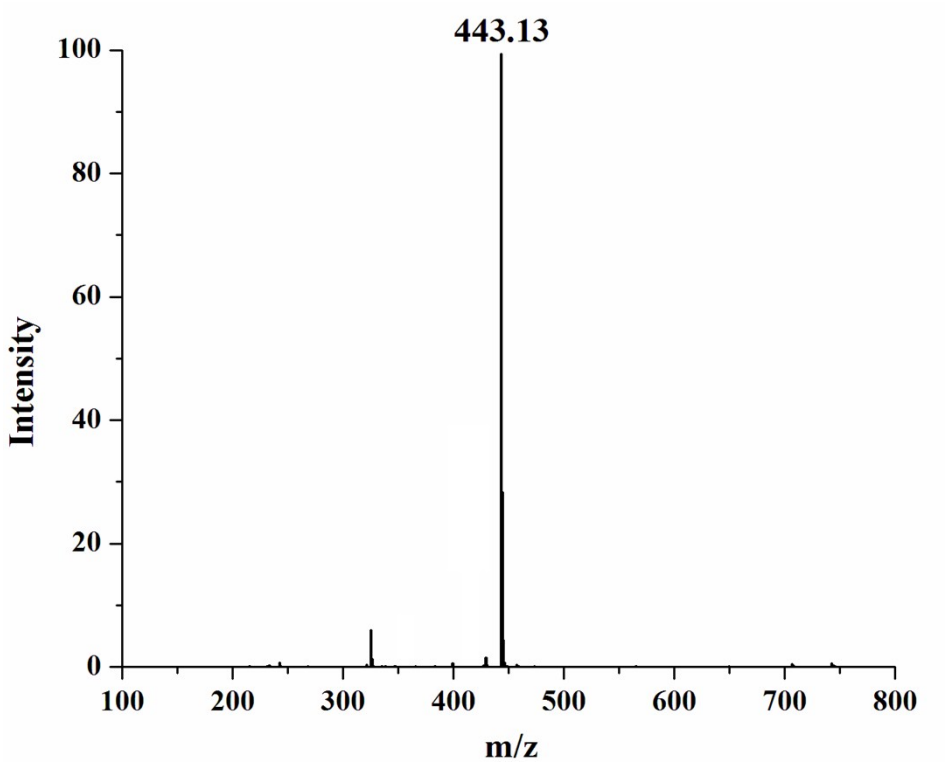

Figure S37. ESI-mass spectrum of complex **4b** in acetonitrile.

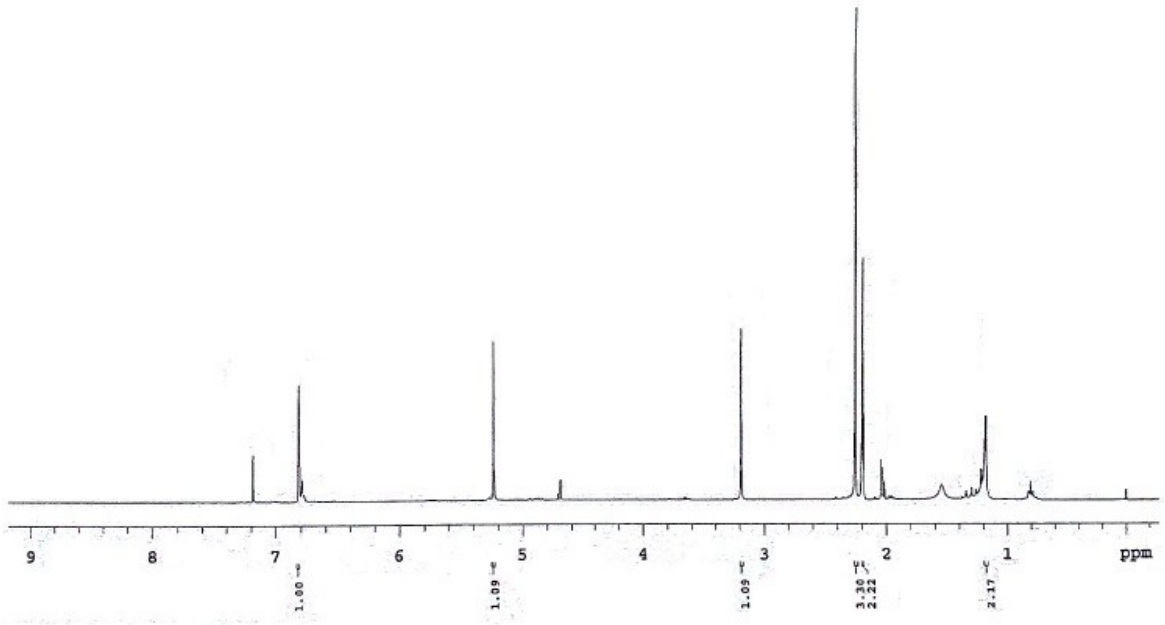

Figure S38. ^{1}H NMR spectrum of modified ligand $\mathbf{L_1}$/ in $CDCl_3$.

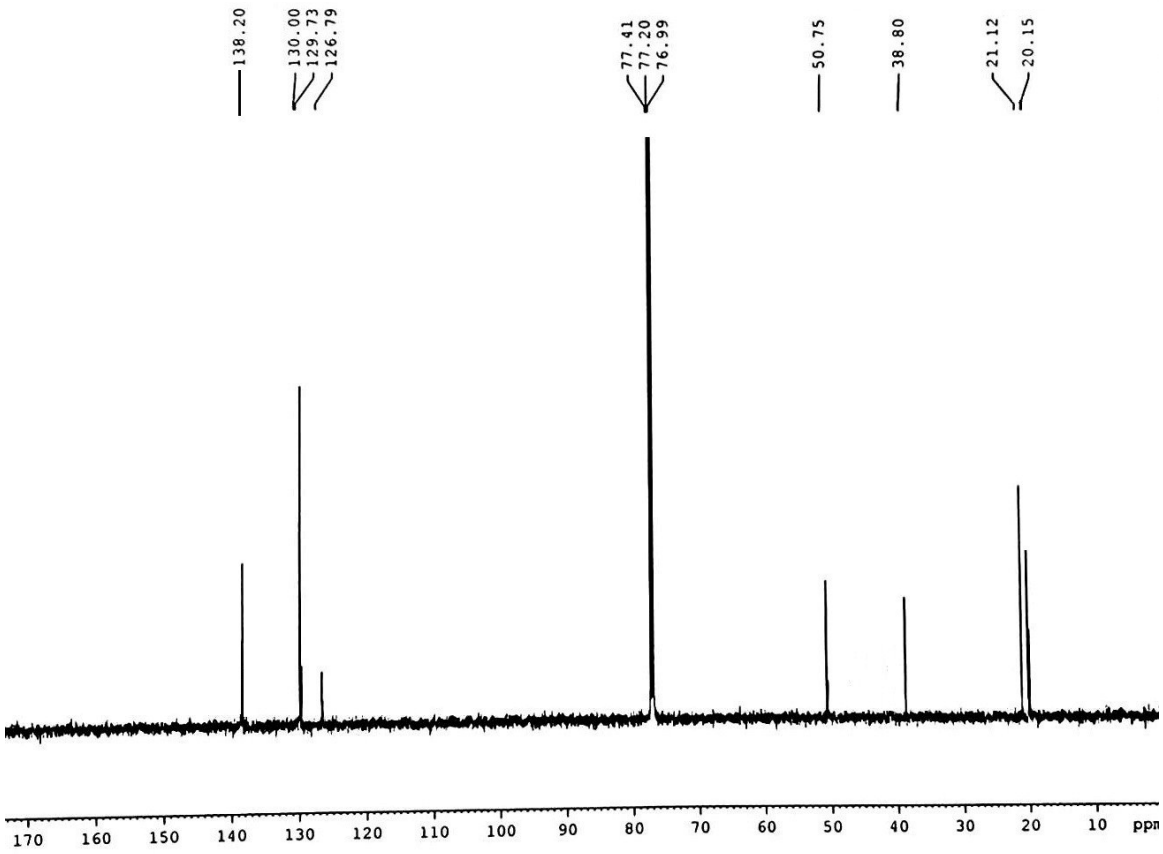

Figure S39. ^{13}C NMR spectrum of modified ligand $\mathbf{L_1}'$ in $CDCl_3$.

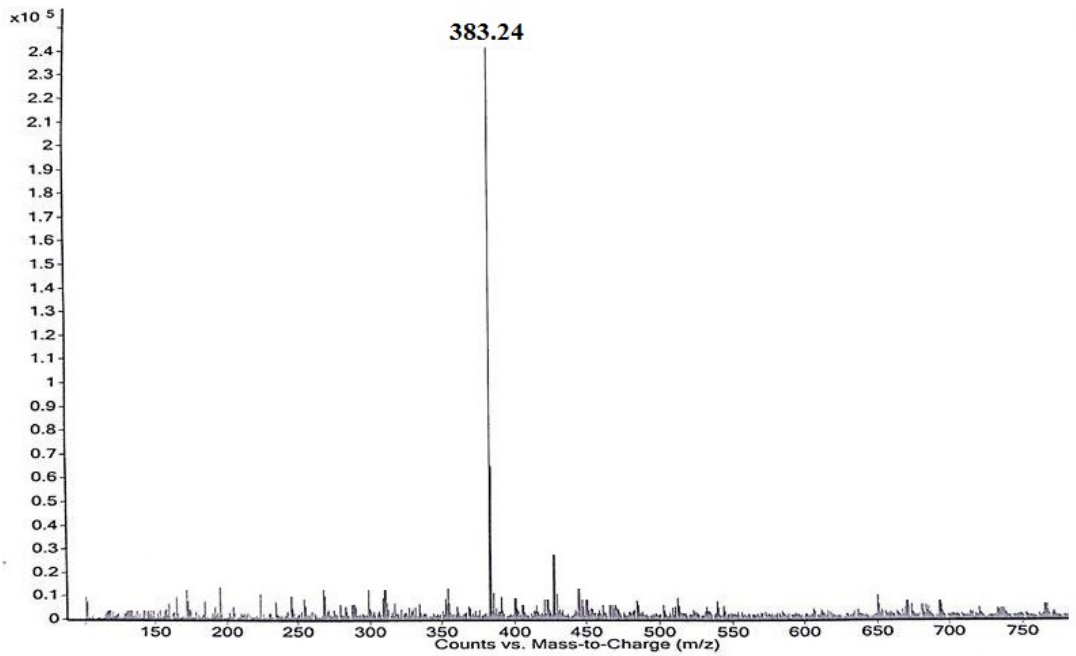

Figure S40. ESI-mass spectrum of modified ligand $\mathbf{L_1}'$ in methanol.

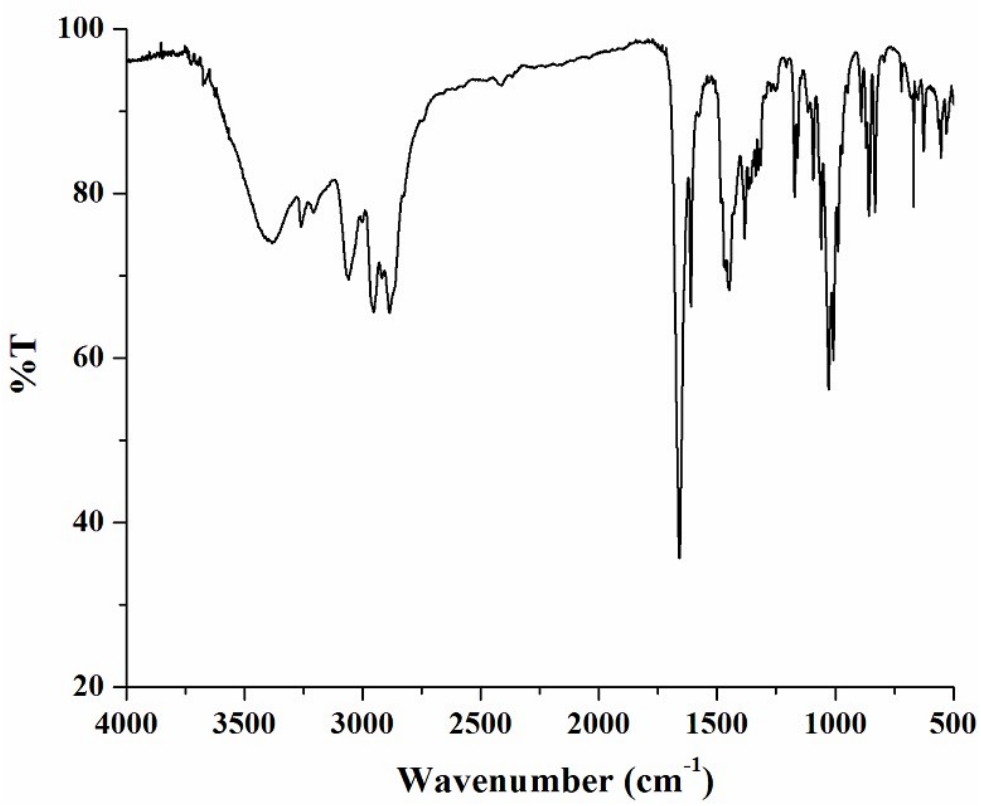

Figure S41. FT-IR spectrum of complex **5** in KBr pellet.

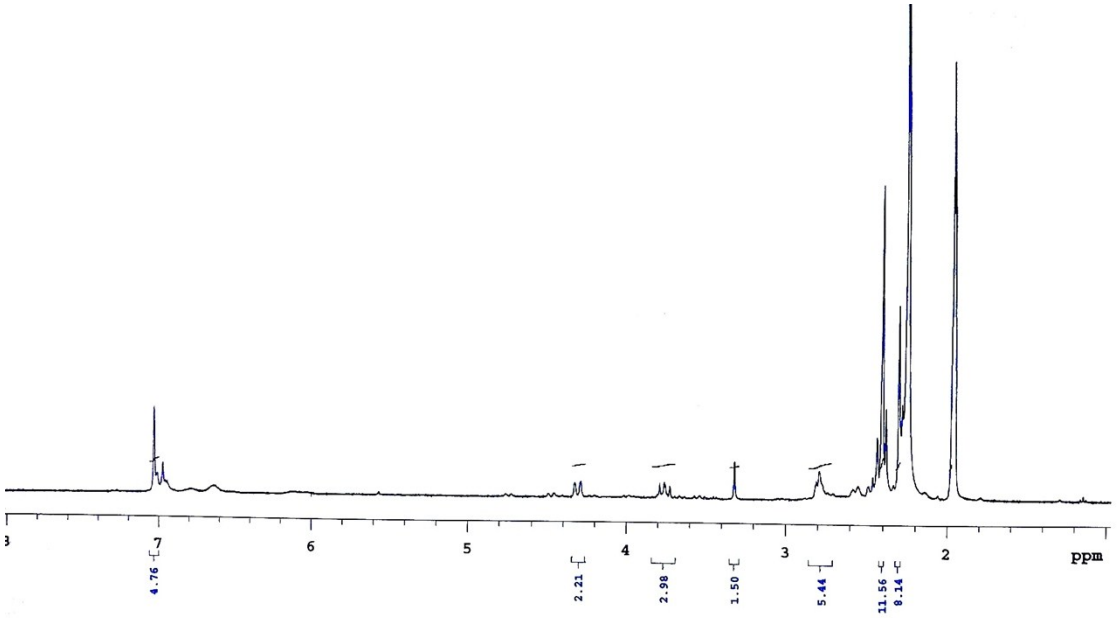

Figure S42. ^{1}H NMR spectrum of complex **5** in CD_3CN.

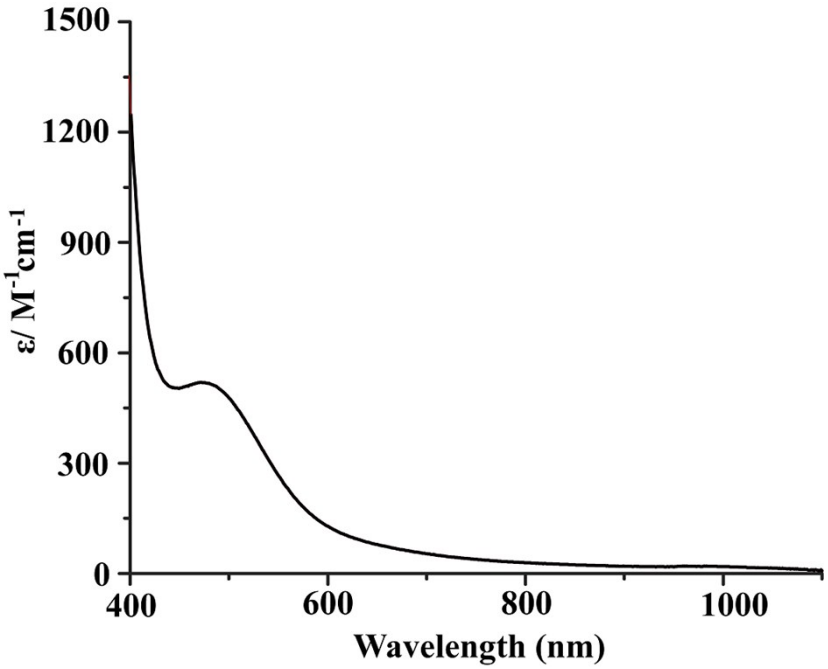

Figure S43. UV-visible spectrum of complex **5** in methanol.

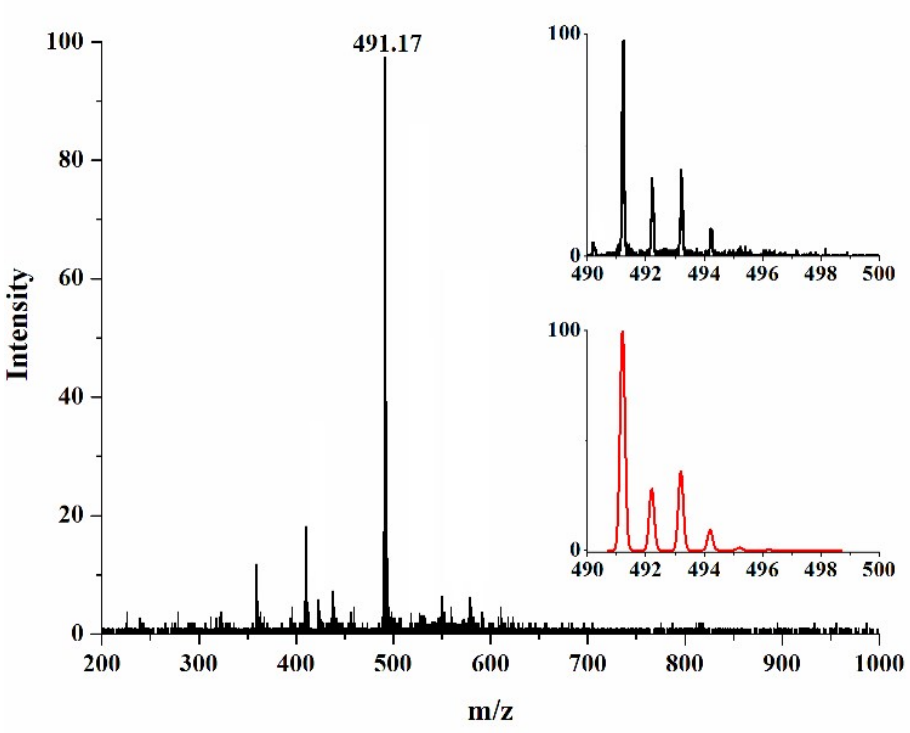

Figure S44. ESI-mass spectrum of complex **5** in acetonitrile. Inset shows isotopic distribution pattern. Black line corresponds experimental and red line corresponds simulated mass spectra.

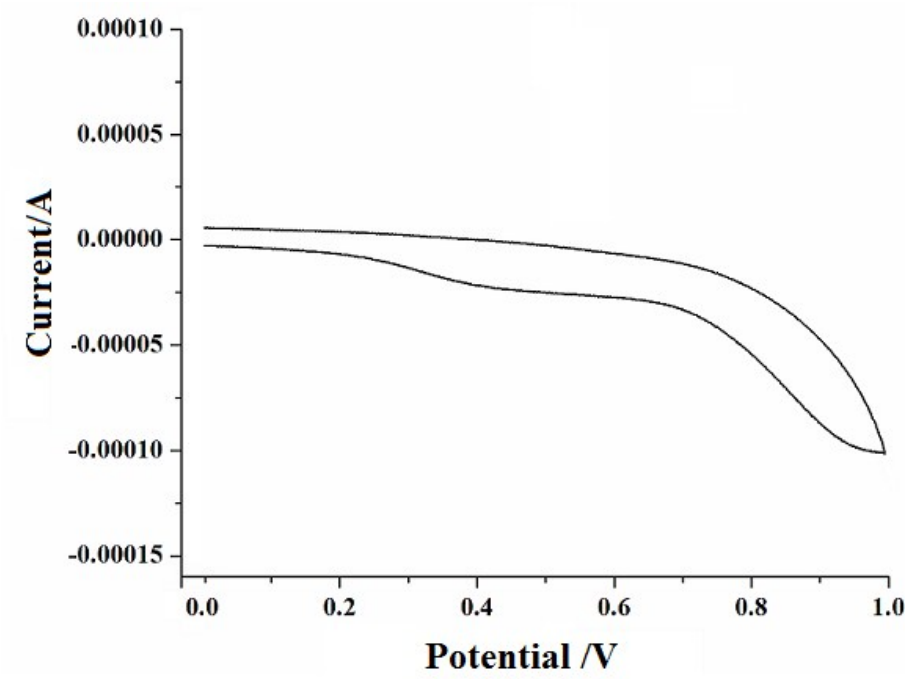

Figure S45. Cyclic Voltammogram of Complex **4a**, positive scan.

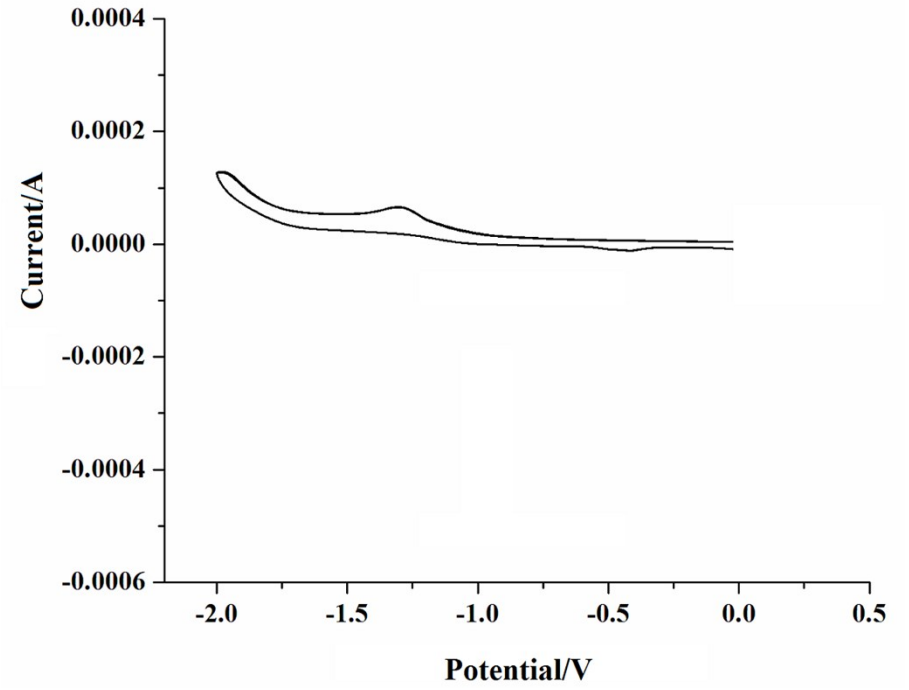

Figure S46. Cyclic Voltammogram of Complex **4a**, negative scan.

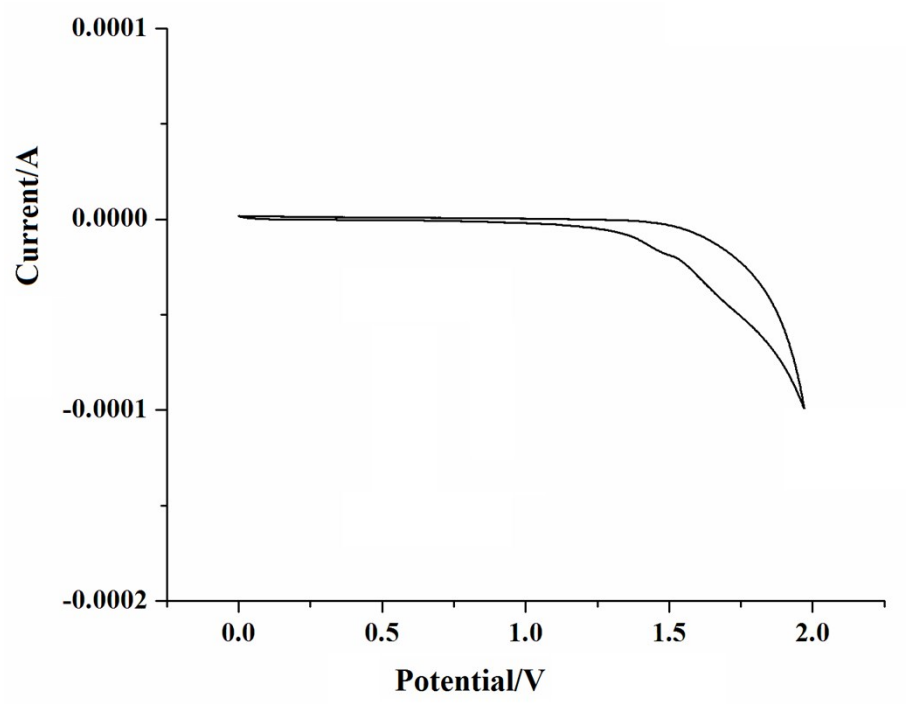

Figure S47. Cyclic Voltammogram of Complex **5**, positive scan.

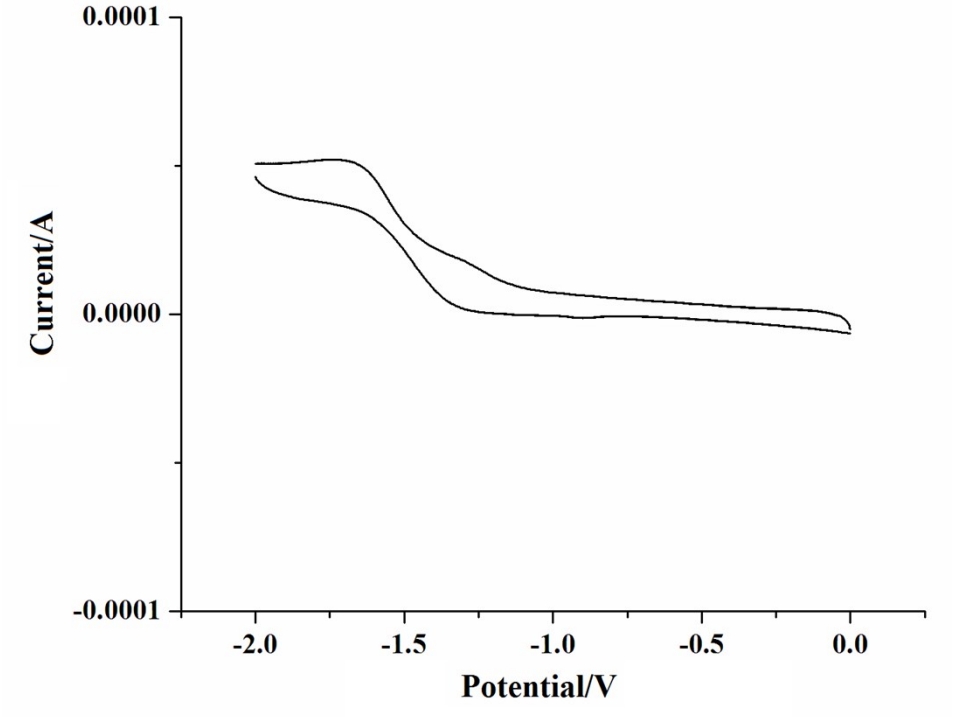

Figure S48. Cyclic Voltammogram of Complex **5**, negative scan.